AIAA 95-2499

Comparative Studies of Convective Heat Transfer Models for Rocket Engines

J.C. DeLise and M.H.N. Naraghi
Department of Mechanical Engineering
Manhattan College
Riverdale, NY 10471

31st AIAA/ASME/SAE/ASEE
Joint Propulsion Conference and Exhibit
July 10-12, 1995/San Diego, CA

Comparative Studies of Convective Heat Transfer Models for Rocket Nozzles

J. C. DeLise* and M. H. N. Naraghi†
Manhattan College, Riverdale, New York 10471

Studies of both numerical and closed-form methods for evaluating the convective heat transfer rates from high temperature combustion gases to the converging-diverging nozzle of a liquid fueled rocket engine are presented. Special attention is given to a numerical model which solves the compressible boundary layer equations and determines the equilibrium composition for the combustion products. The boundary layer equations are solved via an implicit finite-difference scheme. Turbulence closure is obtained using a zero-equation and two-equation model. Results are compared with a semi-empirical closed-form model, and additional numerical model based on conjugate heat transfer. The comparative studies reveal that the computational results are in agreement with the experimental data, and provide improved accuracy in comparison to closed-form solutions.

Nomenclature

A^+ = Van Driest damping constant
h = static enthalpy
l = mixing length
Nu = Nusselt number
P = static pressure
P^+ = dimensionless pressure gradient
P_k = production of turbulence kinetic energy
Pe_t = turbulent Peclet number
Pr = Prandtl number
r = radius of nozzle cross-section
Re_d = Reynolds number based on diameter, du_∞/ν_∞
$Re_{\delta 2}$ = momentum thickness Reynolds number, $\delta_2 u_\infty/\nu_\infty$
u = velocity component in x-direction
u_τ = friction velocity
v = velocity component in y-direction
x = measured distance along the wall surface
y = measured distance normal to the surface

Greek Symbols

δ_1 = displacement thickness
δ_2 = momentum thickness
δ = boundary layer thickness
ϵ = turbulent kinetic energy dissipation rate
μ = dynamic viscosity
ν = kinematic viscosity
ρ = density
τ = shear stress
σ_k = effective Pr number for the turbulence kinetic energy equation
σ_ϵ = effective Pr for the dissipation rate equation

Superscripts and Subscripts

$+$ = dimensionless value
$'$ = fluctuating value
o = stagnation value
t = turbulent value
w = wall value

Introduction

Accurately predicting the convective heat transfer rates from high temperature combustion gases to the nozzle wall is crucial for optimizing the design of thermal control systems in liquid fueled rocket engines. The analysis is especially important for the design of reusable engines which must demonstrate increased life

---

*Graduate Student, Associate Member AIAA
†Professor, Department of Mechanical Engineering, Member AIAA

expectancy. The nozzle of such engines may be more susceptible to reduced fatigue resistance caused by an increased number of temperature cycles.

Preceding the wide availability of high-speed computers and empirical data regarding the nature of the turbulent boundary layer, closed-form Nusselt-Reynolds type correlations were used for computing the convective heat transfer rates between the boundary layer and the wall of the nozzle. These correlation were obtained by fitting formulations based on analytical results to empirically determined heat transfer data. The results obtained with this approach seem to predict heat transfer rates reasonably well for the typical turbulent boundary layer in the nozzle. However, experimental measurements reported by Back et al.[3] show that the convergent and throat sections of the nozzle exhibit heat transfer rates that are less than the rates predicted for the typical turbulent boundary layer. These measurements, and flow observations of Kline,[13] have revealed that the near-wall turbulent portion of the boundary layer transforms to a laminar state under certain conditions. Additional flow field complexities are caused by large favorable pressure gradients, viscous dissipation, variable molecular and turbulent transport properties, and wall curvature. It is in order to acknowledge here that knowledge of the fluid dynamics within the combustion chamber is uncertain, therefore this investigation is restricted to the convergent-divergent nozzle, downstream of this flow behavior.

The numerical model presented is capable of resolving the aforementioned flow field complexities in rocket nozzles. The model is a result of modifying and combining the boundary layer code TEXSTAN[8] with the equilibrium composition code CET.[9,10] TEXSTAN solves the Reynolds-averaged axisymmetric boundary layer equations utilizing an implicit finite difference scheme. The code offers various models for turbulence closure. This investigation will present results for the mixing length and k-ϵ models.

The mixing length model incorporates the Van Driest formulation for inner region prediction. This formulation includes an effective sublayer thickness parameter which responds to changing axial pressure gradient and transpiration. This feature is especially advantageous because boundary layer laminarization is often a consequence of strong favorable pressure gradients which exist in convergent-divergent nozzles.

The k-ϵ turbulence model is the low Reynolds number version developed by Chien.[7] This model is particularly attractive because of it's applicability in the sublayer region. The turbulence transport equations contain damping formulations that enable the finite difference solution to proceed down to the wall surface. This feature eliminates the necessity for matching the k-ϵ model with a wall function in the near-wall region.

The solution of the energy equation is obtained using an algebraic expression for the turbulent Prandtl number. Similar to the mixing length concept, this expression has evolved from analytical and experimental investigations. Although many researchers[5,6] advocate the use of a constant turbulent Prandtl number, the current situation warrants the use of the algebraic expression because of the large temperature gradients expected in the boundary layer.

The code CET computes the equilibrium composition and theoretical rocket performance for the specified reactants and nozzle geometry. These computations employ the following assumptions: one-dimensional flow, complete and adiabatic combustion, zero velocity in the combustion chamber, isentropic expansion, homogeneous mixing, ideal gas, and negligible velocity and temperature variations between condensed and gaseous species. The resulting thermodynamic conditions are then used by the boundary layer code to set the free stream boundary conditions for the solution of the momentum and energy equations. In addition, the equilibrium composition is computed for each transverse node, enabling the determination of the thermodynamic and transport properties. These properties are determined from an extensive data base which has been compiled for numerous rocket engine chemical reactants and products.

Governing Equations

The axisymmetric Reynolds-averaged mass, momentum and stagnation enthalpy equations which govern the boundary layer are written as[7]

$$\frac{\partial}{\partial x}(\rho u r) + \frac{\partial}{\partial y}(\rho v r) = 0 \tag{1}$$

$$\rho u\frac{\partial u}{\partial x} + \rho v\frac{\partial u}{\partial y} = -\frac{dP}{dx} + \frac{1}{r}\frac{\partial}{\partial y}\left[r\left(\mu\frac{\partial u}{\partial y} - \rho\overline{u'v'} \right) \right] \tag{2}$$

$$\rho u\frac{\partial h_o}{\partial x} + \rho v\frac{\partial h_o}{\partial y} = \frac{1}{r}\frac{\partial}{\partial y}\left\{ r\left[\frac{\mu}{Pr}\frac{\partial h_o}{\partial y} - \rho\overline{h_o'v'} + \mu\left(1 - \frac{1}{Pr} \right)\frac{\partial}{\partial y}\left(\frac{u^2}{2} \right) \right] \right\} \tag{3}$$

From the Bousinesq assumption the apparent turbulent stress and heat flux terms are defined by

$$-\overline{u'v'} = \frac{\mu_t}{\rho}\frac{\partial u}{\partial y} \tag{4}$$

and

$$\rho\overline{h_o'v'} = -\frac{\mu_t}{Pr_t}\frac{\partial h}{\partial y} + \rho u\overline{u'v'} \qquad (5)$$

where μ_t and Pr_t represent the turbulent viscosity and Prandtl number.

As mentioned previously, the mixing length and k-ϵ models have selected for this investigation. Mixing length theory employs the following relationship for determining apparent turbulent stress

$$\overline{u'v'} = -l^2\left(\frac{\partial u}{\partial y}\right)^2 \qquad (6)$$

Values for the mixing length l in equation (6), are determined from the empirical relations given below. For the inner region of the turbulent boundary layer, the mixing length is determined from the Van Driest formulation:

$$l = \kappa y\left[1 - \exp\left(-\frac{y^+}{A^+}\right)\right] \qquad (7)$$

where κ represents the *von Kármán constant*. The empirical data of Anderson[1] verifies that κ is approximately 0.41. A^+ in equation (7) is the effective sublayer thickness parameter. The turbulent model includes a formulation for A^+ which is essential for accurately predicting the reduced heat transfer rates associated with boundary layer laminarization. This phenomenon, characterized by a transformation of the near-wall turbulent portion of the boundary layer into a laminar state, occurs in the presence of strong negative streamwise pressure gradients. Laminarization occurs when an acceleration parameter, K exceeds approximately 2×10^{-6} (see reference 11). K is defined as

$$K = \frac{\nu}{u_\infty^2}\frac{du_\infty}{dx} \qquad (8)$$

An empirical relation for A^+, found in Kays and Moffat,[12] is given by

$$A^+ = \frac{25.0}{a\left[v_o^+ + b\left(\frac{p^+}{1 + cv_o^+}\right)\right] + 1} \qquad (9)$$

For flows having constant free stream velocity or favorable pressure gradients $a = 7.1$, $b = 4.25$, and $c = 10.0$.

Since the sublayer exhibits a delayed response to non-equilibrium flow conditions, such as variations in pressure gradient the following rate equation is employed

$$\frac{dA^+}{dx^+} = \frac{A_{eq}^+ - A^+}{C_{lag}} \qquad (10)$$

where $C_{lag} = 4000$.

The mixing length for the outer region is determined as follows

$$l = \lambda\delta_{99} \qquad (11a)$$

for $Re_{\delta_2} > 5500$ and

$$l = \frac{2.942\,\lambda}{Re_{\delta_2}^{0.125}\left[1 - 67.5\frac{(\dot{m}_w''/\rho_w)}{u_\infty}\right]} \qquad (11b)$$

for $Re_{\delta_2} \le 5500$, where $\lambda = 0.085$.

The turbulent Prandtl number in equation (5) is determined from the following expression

$$Pr_t = \left\{\frac{1}{2Pr_{t_\infty}} + \frac{0.3Pe_t}{Pr_{t_\infty}^{1/2}} - (0.3Pe_t)^2\left[1 - \exp\left(-\frac{1}{0.3Pe_t Pr_{t_\infty}^{1/2}}\right)\right]\right\}^{-1} \qquad (12)$$

The reasoning behind equation (12) as well as the empirical data from which it was derived is described in Kays and Crawford.[11]

The second turbulence model used is a low-Reynolds number k-ϵ model formulated by Chien.[7] The axisymmetric form of the turbulence kinetic energy transport equation is written as

$$\rho u\frac{\partial k}{\partial x} + \rho v\frac{\partial k}{\partial y} = \frac{1}{r}\frac{\partial}{\partial y}\left(r\mu_k\frac{\partial k}{\partial y}\right) + P_k - \rho\epsilon - \frac{2\mu k}{y^2} \qquad (13)$$

where

$$\mu_k = \mu + \mu_t/\sigma_k, \qquad \mu_t = c_\mu f_\mu \rho k^2/\epsilon, \qquad c_\mu = 0.09$$

$$f_\mu = 1 - \exp(-0.0115y^+), \qquad \sigma_k = 1$$

The dissipation rate transport equation is written as

$$\rho u\frac{\partial \epsilon}{\partial x}+\rho v\frac{\partial \epsilon}{\partial y}$$

$$=\frac{1}{r}\frac{\partial}{\partial y}\left[r\mu_{\epsilon}\frac{\partial \epsilon}{\partial y}\right]+c_{\epsilon 1}\frac{\epsilon}{k}P_k-c_{\epsilon 2}f_{\epsilon 2}\rho\frac{\epsilon^2}{k}-\frac{2\mu f_{\epsilon}\epsilon}{y^2} \quad (14)$$

where

$$\mu_{\epsilon}=\mu+\mu_t/\sigma_{\epsilon},\quad \sigma_{\epsilon}=1.3,\quad c_{\epsilon 1}=1.35,\quad c_{\epsilon 2}=1.8$$

$$f_{\epsilon}=\exp(-0.5y^{+})$$

$$f_{\epsilon 2}=1-0.222\exp[-(\rho k^2/6\mu\epsilon^2]$$

The terms μ_t and μ_{ϵ} represent the sum of the laminar and turbulent viscosities for equations (13) and (14). The production of turbulence kinetic energy P_k is defined as

$$P_k=\mu_t\left(\frac{\partial u}{\partial y}\right)^2$$

Numerical Solution

Finite-Difference Scheme

The derivation of the finite-difference equations, originally formulated by Patankar and Spalding[16] is accomplished by expressing each of the individual terms in equations (2), (3), (13) and (14) as an integrated average over a two-dimensional finite-control volume. The advantage offered by this approach, in comparison to substituting a Taylor series expansion for each term in the partial differential equation, is that it guarantees that the conservation equations will be satisfied over the computational domain of the problem. Since the partial differential equations are parabolic, space-marching in the streamwise direction is employed. Hence, the integral equation corresponding to each tranverse node is evaluated at the downstream station. The resulting algebraic equation for each transverse node is written in terms of adjacent nodes and the known upstream value, forming a tridiagonal system of equations which are solved using a successive-substitution algorithm.

Although the finite-difference scheme is only first-order accurate in the streamwise direction, the stable nature of this implicit scheme is a considerable asset. The coefficients in the finite-difference equations are evaluated at the upstream station, where the values of the dependent variables are known. This strategy, commonly referred to as "lagging" the coefficients, decouples the finite-difference representation of the governing equations, permitting each to be marched independently. Mutual dependence between these equations is established by updating the coefficients after each marching step. A detailed derivation of the finite-difference equations is documented in reference 16.

Equilibrium Composition Analysis

Using the existing computational framework in the driver program of TEXSTAN, the equilibrium composition code is called to: 1) establish the free-stream thermodynamic conditions for all stations specified in the input data set, and 2) determine the fluid properties for nodes within the boundary layer. For both procedures the equilibrium composition is computed by minimizing the Gibbs free energy in conjunction with an iterative technique (see reference 9).

The free-stream thermodynamic conditions for a convergent-divergent nozzle are determined by specifying the combustion chamber pressure, nozzle geometry, and oxygen-fuel ratio (the reactant enthalpies are provided by a data base in the code). Here the mixture enthalpies and the corresponding temperatures, pressures, and Mach numbers are determined using the assumptions associated with theoretical rocket performance for equilibrium compositions. Recall that these assumptions were identified in the introduction of this paper.

The original version of TEXSTAN contains a subroutine that provides the thermodynamic and molecular transport properties for the fluid being considered by a given problem. However, this subroutine cannot handle high temperature gases and reacting flows. This subroutine has been replaced by the subroutines THERMP and TRANP which are imbedded in equilibrium composition code. As characterized by their names, these subroutines are used to evaluate the thermodynamic and molecular transport properties for products of combustion which contain multiple gas species having temperatures as high as 9000 °R (5000 K). The properties of each species are determined from least squares curve fitted experimental data. Hence, the data files contain the coefficients for the polynomials which correspond to a given chemical species.

Results and Discussion

High Temperature Air

Before presenting the results of the combined codes, the original form of TEXSTAN will be used to investigate experimental results obtained for two convergent-divergent nozzles.

The analysis of the first convergent-divergent nozzle is based on the data reported by Back et al.[2] This

experimental data was obtained for heated-air flowing through a cooled nozzle where the stagnation temperature and pressure were 1518°R and 75 psia, respectively. The configuration of this nozzle as well as the experimentally determined wall temperature isotherms are presented in Figure 1. From these isotherms the local heat flux can be determined, which can then be used to compute the convective heat transfer coefficient h_c along the wall. A comparison of these values with h_c predicted by TEXSTAN and a closed-form semi-empirical N-R (Nusselt-Reynolds) correlation is presented in Figure 2. As previously described, the N-R correlation is obtained by fitting formulations based on intuitive and analytical results to empirically determined heat transfer data for nozzles. This correlation is defined as[4]

$$Nu = C\ Re_D^{0.8} Pr^{0.4} \qquad (15)$$

where the correlation coefficient C is equal to 0.026. Notice that the heat transfer coefficient near the throat is over-predicted by both TEXSTAN and the N-R correlation by approximately 20% and 70%, respectively. Since the N-R correlation fares better for other sections of the nozzle, it becomes apparent that this approach does not account for the laminarization of the turbulent portion of the boundary layer. As previously mentioned, laminarization is dominant in the vicinity of the throat and causes reduced heat transfer rates in this region.

The second analysis is based on the data reported by Kolozsi.[14] The fluid used for these tests was air and the stagnation temperature and pressure were 1215°R and 370 psia, respectively. The wall temperatures were maintained at 50 to 55 percent of the stagnation temperature. Because of this small variation, the wall temperatures specified in the input data set were held constant. Figure 3 compares the experimentally determined values of h_c with those predicted by TEXSTAN and the N-R correlation. Similar to the results obtained for the previous nozzle, the code and the N-R correlation over-predict the heat transfer coefficient at the throat by approximately 25% and 65%, respectively.

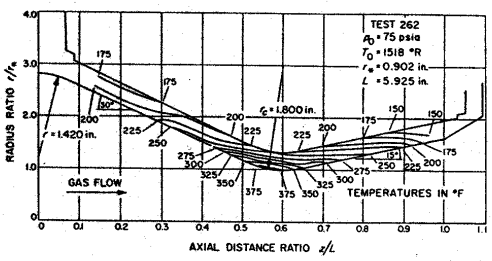

Figure 1: Configuration of the nozzle investigated by Back et al.[2].

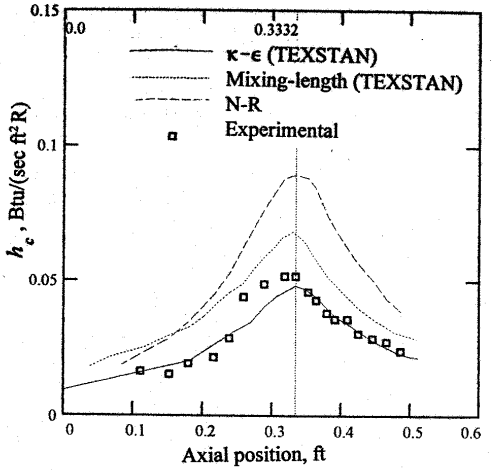

Figure 2: A comparison of heat transfer coefficients based on different models for the nozzle configuration shown in Figure 1.

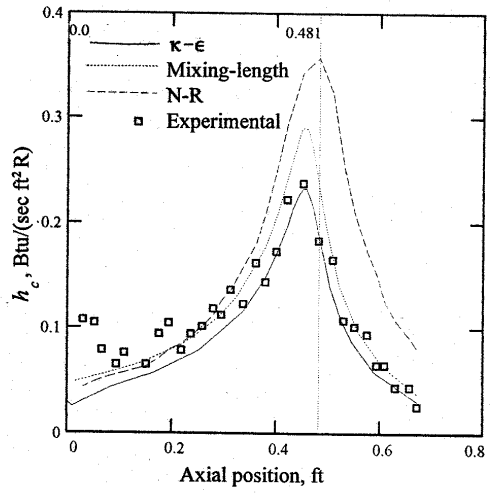

Figure 3: A comparison of heat transfer coefficients based on different models for the nozzle reported in reference 14.

TEXSTAN appears to be in excellent agreement with experimental data in the convergent and divergent sections.

For both nozzles, the experimental data and the results obtained using TEXSTAN reveal a delay between thermal response and laminarization (as shown by Figures 2 and 3, the N-R correlation does not accurately predict this

behavior). In other words, the reduced heat transfer rates associated with laminarization occur downstream of the largest values of K.

Combustion Gases

Results were obtained for a rocket engine burning a stoichiometric mixture of hydrogen and oxygen, and having a combustion chamber pressure of 1000 psia. These results were compared with the numerical results of the RTE (Rocket Thermal Evaluation) code developed by Naraghi.[15] This code evaluates both the convective (using a N-R type correlation) and radiative heat transport between the high temperature gases and the interior wall of the nozzle, and also incorporates a model to account for the heat removed by the regenerative cooling system in the nozzle wall. The contribution made by radiation is considered to be minimal because the combustion products resulting from the hydrogen-oxygen reaction are non-luminous. This is not the case for hydrocarbon fuels, where the formation of soot can double or triple the heat radiated by combustion products. A comparison of the heat flux predicted by RTE and the modified version of TEXSTAN is presented in Figure 4. Although, this comparison is not based on experimental results, it is considered to be accurate because of the conjugate heat transfer model used in RTE. Similar to the previous experimentally based analyses, there is a significant deviation near the throat which again may be attributed to the inability of the N-R type correlation to account for the reduced heat transfer rates associated with laminarization. The results from the modified version of TEXSTAN indicate that the acceleration parameter K is greater than 2×10^{-6} in the throat region; therefore, verifying the existence of laminarization. As shown by Figure 4, the results for the two numerical models agree very well with each other in convergent and divergent sections.

Finally, consideration is given to a rocket nozzle investigated experimentally at the Jet Propulsion Laboratory[17]. The fuel and oxidizer for this engine were hydrazine and nitrogen tetroxide, respectively. Testing was conducted with a combustion chamber pressure of 199 psia and a nozzle wall temperature of 860 °R. Figure 5 compares the experimental and predicted heat flux. The predicted values are computed with the modified version of TEXSTAN using the mixing length turbulence model. The numerical model appears to be overpredicting the heat flux by approximately 35%. Similar to the high-temperature air experiments, shows a delay between thermal response and laminarization.

Conclusion

The results presented in this paper confirm that numerical analysis of the boundary layer code predicts heat transport more accurately than the semi-empirical N-R correlation. The large improvements in accuracy obtained for the region near the throat verifies the need to accurately model the effects of boundary layer laminarization. In reference to the turbulence models, the k-ϵ model demonstrates excellent agreement when compared to the experimental data. However, the mixing length model fares better for predicting the delay between thermal response and laminarization.

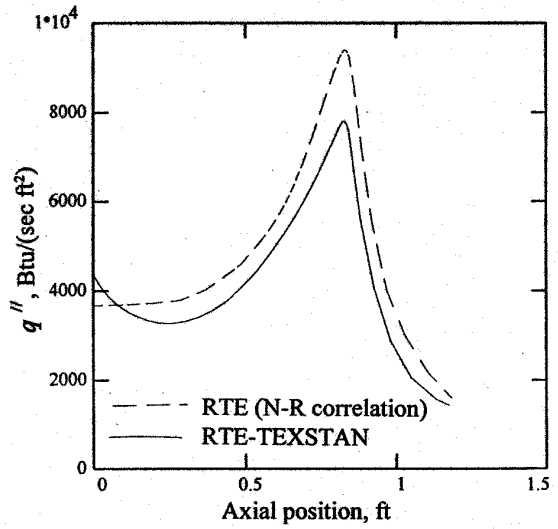

Figure 4: Comparison of wall heat fluxes evaluated based on RTE (N-R correlation) and RTE-TEXSTAN.

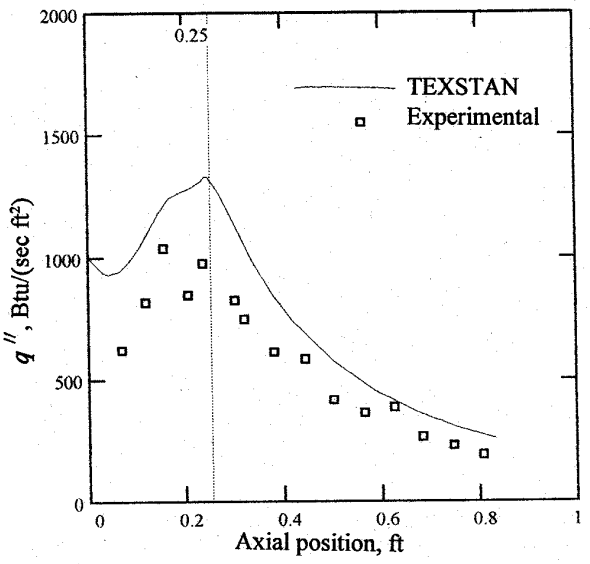

Figure 5: Comparison of experimental and RTE-TEXSTAN results for the nozzle reported in reference 17.

Acknowledgment

The authors would like to express their gratitude to Dr. Michael E. Crawford at The University of Texas for providing us with a copy of the computer code, TEXSTAN, and for his generous assistance in enhancing our understanding of the complexities of this code.

References

[1]Anderson, P. S., Kays, W.M., and Moffat, R. J., *Journal of Fluid Mechanics*, Vol. 69, 1975, pp. 353-375.

[2]Back, L. H., Massier, P. F., and Gier H. L., "Convective Heat Transfer in a Convergent-Divergent Nozzle", *International Journal of Heat and Mass Transfer*, Vol. 7, 1964, pp. 549-568.

[3]Back, L. H., Cuffel, R. F., and Massier, P. F., "Laminarization of a Turbulent Boundary Layer in Nozzle Flow - Boundary Layer and Heat Transfer Measurements with Wall Cooling", *Journal of Heat Transfer Series C*, Vol. 92, 1970, p. 333.

[4]Bartz, D.R.,"Turbulent Boundary_layer Heat Transfer from Rapidly Accelerating Flow of Rocket Combustion Gases and of Heated Air," Advances in Heat Transfer, pp. 2-108, 1965.

[5]Boyle, R. J., "Navier-Stokes Analysis of Turbine Blade External Heat Transfer," ASME Paper 90-GT-42, 35th ASME Gas Turbine and Aeroengine Conference and Exposition, Brussels, 1990.

[6]Cebeci, T., and Smith, A. M. O., *Analysis of Turbulent Boundary Layers*, Academic Press, New York, 1974.

[7]Chien, K. Y., "Predictions of Channel and Boundary Layer Flows with a Low-Reynolds-Number Turbulence Model," *AIAA Journal*, Vol. 20, Jan. 1982, pp. 33-38.

[8]Crawford, M. E., TEXSTAN - Boundary Layer Finite-Difference Computer Code, academic version, Thermal/Fluids Systems Group of the Mechanical Engineering Department, The University of Texas at Austin, April 1994.

[9]Gordon, S., and Mcbride, B. J., "Computer Program for Calculation of Complex Chemical Equilibrium Compositions, Rocket Performance, Incident and Reflection Shocks, and Chapman-Jouquet Detonations", NASA SP-270, 1971.

[10]Gordon, S., Mcbride, B. J., and Zeleznik, F. J., "Computer Program for Calculation of Complex Chemical Equilibrium Compositions and Applications Supplement I -Transport Properties", NASA TM-86885, October 1984.

[11]Kays, W. M., and Crawford, M. E., *Convective Heat and Mass Transfer*, Third Edition McGraw-Hill, New York, 1993.

[12]Kays, W. M., and Moffat, R. J., *Studies in Convection*, Vol. 1, Academic Press, London, 1975.

[13]Kline, S. J., "Observed Structural Features in Turbulent and Transitional Boundary Layers", *Fluid Mechanics of Internal Flow*, ed. G. Sovran, Elsevier, Amsterdam, 1967.

[14]Kolozsi, J. J., "An Investigation of Heat Transfer through the Turbulent Boundary Layer in an Axially Symmetric, Convergent-Divergent Nozzle", Masters Thesis, Dept. of Aeronautical and Astronautical Engineering", Ohio State University, 1985.

[15]Naraghi, M. H. N., "RTE - A Computer Code for Three-Dimensional Rocket Thermal Evaluation", Revision 2, Prepared for the National Aeronautics and Space Administration, Grant 3-892, 1991.

[16]Patankar, S. V., and Spalding D. B., *Heat and Mass Transfer in Boundary Layers*, First Edition, Morgan-Grampian, London, 1967.

[17]Witt, A.B., and Harper, E.Y., "Experimental Investigation and Empirical Correlation of Local Heat Transfer Rates in Rocket-Engine Thrust Chambers," Technical Report No. 32-244, Jet Propulsion Lab., California Institute of Technology, Pasadena, Calif., March 19, 1962.